hexagon:2611.00349v2

Cross-Energy of Dirichlet Partial Sums. Part 33: Optimised mollifiers and the bound $\Lambda \leq 0.174$ for the de Bruijn–Newman constant

Pedro Caceres
Universidad Europea de Valencia
pedrojesus.caceres@universidadeuropea.es

Version 3, 12 November 2026 (renumbered 2 Nov 2026, formerly Part 13)
Proof material (weights, certificate scripts, complete logs of both runs):
https://doi.org/10.5281/zenodo.XXXXXXXX
Part 33 of the book-series *Cross-Energy of Dirichlet Partial Sums* (forty-seven parts, Parts 0–46; block VI: The de Bruijn–Newman constant). Part 0 is the guide. In book version 1 (2 November 2026) this was Part 30; the present numbering is that of book version 2 (10 November 2026).

Abstract

The Polymath project reduced upper bounds for the de Bruijn–Newman constant Λ to three verifiable hypotheses: the Riemann hypothesis up to height $X/2$, a zero-free region for H_{t_0} to the right of X, and a barrier at X. With the verification of the Riemann hypothesis up to $3 \cdot 10^{12}$ by Platt and Trudgian, this gave $\Lambda \leq 0.2$. The bottleneck is the zero-free region, which Polymath established with Euler-product mollifiers. We replace the Euler product by a mollifier $\sum_{d \leq D} \lambda_d d^{-s_*}$ whose weights are chosen by solving an ℓ^1-regression problem, so that any choice of weights still yields a valid lower bound. At the same height $X \approx 6 \cdot 10^{12}$ and $t_0 = 0.155$, $y_0 = 0.2$, the lower bound for the mollified sum improves from -0.12 (our Lemma 3 evaluated with the Euler mollifier on the primes up to 13) to $+0.05$ with $D = 120$; with $D = 240$ it is still $+0.04$ at $t_0 = 0.154$. We cover all $x \geq X$ by a short chunking argument together with a tail estimate, verify the barrier with Polymath's Taylor scheme, and obtain

$$\Lambda \leq 0.174.$$

The certificates are computer-assisted. They use Arb ball arithmetic for all transcendental functions and outward-rounded floating-point arithmetic for the large sums. The code, the weights and the complete logs of both runs are publicly archived in a version-specific record (Data and code), and the certificate was reproduced on a second platform. We also report that at this height the weights we found with $D = 240$ do not reach 0.173, and we compare with Polymath's table of conditional results. We do not prove the Riemann hypothesis.

MSC 2020: 11M26 (primary); 11Y35, 30D10.

1 Introduction

Let $H_t(z) = \int_0^\infty e^{tu^2} \Phi(u) \cos(zu)\, du$ with $\Phi(u) = \sum_{n \geq 1} (2\pi^2 n^4 e^{9u} - 3\pi n^2 e^{5u}) e^{-\pi n^2 e^{4u}}$, so that $H_0(z) = \frac{1}{8}\xi(\frac{1}{2} + \frac{iz}{2})$. De Bruijn showed that H_t has only real zeros for $t \geq \frac{1}{2}$ and that this property persists as t increases [dB]; Newman showed that there is a constant $\Lambda \leq \frac{1}{2}$ such that H_t has

only real zeros exactly when $t \geq \Lambda$ [Ne]; Ki, Kim and Lee proved $\Lambda < \frac{1}{2}$ [KKL]. The Riemann hypothesis (RH) is equivalent to $\Lambda \leq 0$, and Rodgers and Tao proved $\Lambda \geq 0$ [RT]. Polymath proved $\Lambda \leq 0.22$ [Pm], and the verification of RH up to $3 \cdot 10^{12}$ by Platt and Trudgian gave $\Lambda \leq 0.2$ [PT], who remarked that "some extra decimals could be wrought out of the calculation". In 2026 Gomila announced $\Lambda \leq 0.1787854$ with interval certificates, using Euler mollifiers on the primes up to 11 [Go]. Several further claims have appeared since, none of them refereed at the time of writing. Gordon announced $\Lambda < 0.158$, combining the theorem of Platt and Trudgian with new analytic estimates and interval computations [Gor]. OpenAI released a manuscript, with a partial Lean formalization, claiming that ζ has no zeros with real part greater than $\frac{7}{8}$ [OAI]; by de Bruijn's theorem [dB, Thm. 13] such a half-plane alone gives $\Lambda \leq \frac{1}{2}(\frac{3}{4})^2 = \frac{9}{32}$, a consequence that has been formalized in Lean [Mu], and Hakimoglu-Brown obtains $\Lambda \leq 0.13963$ under the same hypothesis [HB]. Planat obtained a certified comparison $\Lambda < 0.148612$ under three analytic premises that are not yet established [Pl]. The present paper is unconditional, uses only the criterion of Polymath and the height verified by Platt and Trudgian, and does not depend on any of these claims; its contribution is a method, the optimisation of the mollifier, together with a certificate; it is not the smallest value that has been announced. Lower bounds go the other way: by Part 35 of this series [CE35], a hypothetical zero $\frac{1}{2} + \delta + i\gamma$ of ζ with $\delta > 0$ (which must have $\gamma > 3 \cdot 10^{12}$) forces $\Lambda \geq \delta^2/(70 \log \gamma \log\log \gamma)$.

All these results use the criterion of Polymath, recalled in Theorem 2 below. Its hypothesis (ii), a zero-free region for H_{t_0} to the right of X, is the bottleneck [Pm, Sect. 1]: it requires a lower bound for a Dirichlet-type sum f_{t_0} that is valid on a whole torus of phases, and the triangle inequality is too weak without a mollifier. Our only new idea is to stop prescribing the mollifier and to optimise it. For any real weights λ_d with $\lambda_1 = 1$, the inequality of Lemma 3 gives a lower bound, so the weights can be chosen by a convex optimisation (an ℓ^1 regression) without any loss of rigour. The optimal weights differ substantially from an Euler product (Figure 1).

Theorem 1 (computer-assisted)**.** $\Lambda \leq 0.15399 + \frac{1}{2}(0.2)^2 = 0.17399 < 0.174$.

Table 1 puts this in context. At the same height $X \approx 6 \cdot 10^{12}$, Polymath's conditional table [Pm, Table 1] lists $\Lambda \leq 0.20$, and suggests that 0.18 would need $X \approx 6 \cdot 10^{13}$ and 0.17 would need $X \approx 3 \cdot 10^{14}$.

source	RH verified to	mollifier	bound
Polymath 2019 [Pm]	$3.06 \cdot 10^{10}$	Euler	$\Lambda \leq 0.22$
Platt–Trudgian 2021 [PT]	$3 \cdot 10^{12}$	Euler (Polymath table)	$\Lambda \leq 0.2$
Gomila 2026 (announcement) [Go]	$3 \cdot 10^{12}$	Euler, $p \leq 11$	$\Lambda \leq 0.1787854$
this paper	$3 \cdot 10^{12}$	optimised, $d \leq 240$	$\Lambda \leq 0.174$

Table 1: Upper bounds for Λ obtained with Polymath's criterion and the height of Platt and Trudgian, with no further hypothesis. The claims of [Gor] (new analytic estimates), [HB] (conditional on the half-plane of [OAI]) and [Pl] (conditional on three analytic premises) are discussed in the introduction.

Place in the book. This is Part 33 of the series, in block VI (the de Bruijn–Newman constant). It builds on Part 1 (the cross-energy of the partial sums), Part 6 (the prime phases and the second-order energy), Part 18 (the Dirichlet-polynomial mollifier of the Euler–Caceres bound) and its two companions in the block, Parts 34 and 35. It is used by Parts 34 and 35 and is cited in Parts 2, 8 and 17.

2 The Polymath criterion and the effective approximation

Theorem 2 ([Pm, Thm. 1.2]). *Let $t_0, X > 0$ and $0 < y_0 \le 1$, and assume: (i) $\zeta(\sigma+iT) \ne 0$ for $\frac{1+y_0}{2} \le \sigma \le 1$ and $0 \le T \le X/2$; (ii) $H_{t_0}(x+iy) \ne 0$ for $x \ge X + \sqrt{1-y_0^2}$ and $y_0 \le y \le \sqrt{1-2t_0}$; (iii) $H_t(x+iy) \ne 0$ for $X \le x \le X + \sqrt{1-y_0^2}$, $\sqrt{y_0^2 + 2(t_0-t)} \le y \le \sqrt{1-2t}$ and $0 \le t \le t_0$. Then $\Lambda \le t_0 + \frac{1}{2}y_0^2$.*

We take $t_0 = 0.15399$, $y_0 = 0.2$ and $X = 5\,998\,313\,329\,980.3135$. Then $X/2 < 3 \cdot 10^{12}$ and (i) is the theorem of Platt and Trudgian [PT]. The location of X was chosen, as in [Pm, Sect. 8.1], to make the partial Euler product $\prod_{p \le 13} |1-p^{-s}|^{-1}$ large at $s = 0.6 - iX/2$; this keeps $|f_t|$ large on the barrier.

In the region $0 < t \le \frac{1}{2}$, $0 \le y \le 1$, $x \ge 200$, Polymath [Pm, Thm. 1.3] write $H_t/B_t = f_t + O_{\le}(e_A + e_B + e_{C,0})$ with

$$f_t(x+iy) = \sum_{n=1}^{N} \frac{b_n}{n^{s_*}} + \gamma \sum_{n=1}^{N} \frac{n^y b_n}{n^{\overline{s_*}+\kappa}}, \qquad b_n = e^{\frac{t}{4}\log^2 n}, \qquad N = N_{\mathrm{Pm}}(x) := \Big\lfloor \sqrt{\tfrac{x}{4\pi} + \tfrac{t}{16}} \Big\rfloor,$$

where s_*, κ, γ are explicit, and they prove the explicit bounds

$$|\gamma| \le e^{0.02y} \Big(\frac{x}{4\pi}\Big)^{-y/2}, \quad \operatorname{Re} s_* \ge \frac{1+y}{2} + \frac{t}{4}\log\frac{x}{4\pi} - \frac{t}{x^2}, \quad |\kappa| \le \frac{ty}{2(x-6)}, \tag{1}$$

(their (20)–(22); we have simplified the last term of (21) using $x \ge 200$), together with explicit bounds (23), (24) for $e_A + e_B$ and $e_{C,0}$. Then $|f_t| > e_A + e_B + e_{C,0}$ implies $H_t \ne 0$ [Pm, Cor. 1.4]. At our height $e_A + e_B + e_{C,0} \le 3 \cdot 10^{-7}$ throughout region (ii).

3 Optimised mollifiers

Write $f_t = A + \gamma B$ with $A = \sum_{n \le N} b_n n^{-s_*}$ and $B = \sum_{n \le N} n^y b_n n^{-\overline{s_*}-\kappa}$, and let $\sigma = \operatorname{Re} s_*$.

Lemma 3. *Let $\lambda_1 = 1$ and $\lambda_2, \dots, \lambda_D \in \mathbb{R}$, and put*

$$c_n = \sum_{\substack{d \mid n,\ d \le D \\ n/d \le N}} \lambda_d\, b_{n/d}, \qquad c_n'(y) = \sum_{\substack{d \mid n,\ d \le D \\ n/d \le N}} \lambda_d\, d^{-y} b_{n/d}.$$

Then, with

$$\mathcal{L} = 1 - \sum_{n \ge 2} |c_n| n^{-\sigma} - |\gamma| \sum_{n \ge 1} \big(|c_n'(y)| + \epsilon_n\big) n^{y-\sigma+|\kappa|}, \qquad \epsilon_n = \sum_{\substack{d \mid n,\ d \le D \\ n/d \le N}} |\lambda_d| d^{-y} b_{n/d}\,(D^{|\kappa|} - 1),$$

$$|f_t| \ \ge\ |A| - |\gamma||B| \ \ge\ \frac{\mathcal{L}}{\sum_{d \le D} |\lambda_d| d^{-\sigma}} \qquad \text{whenever } \mathcal{L} > 0.$$

Proof. All sums are finite: $d \le D$, $m \le N$ and $n = dm \le DN$. For real $u > 0$ and complex w we write $u^w = e^{w \log u}$, so that $u^w u^{w'} = u^{w+w'}$, $\overline{u^w} = u^{\bar w}$ and $|u^w| = u^{\operatorname{Re} w}$. The numbers $b_m = e^{\frac{t}{4}\log^2 m}$ are real and positive, and $b_1 = 1$.

Step 1 (the mollifier). Put $M = \sum_{d \le D} \lambda_d d^{-s_*}$. Then $|M| \le M^+ := \sum_{d \le D} |\lambda_d| d^{-\sigma}$.

Step 2 (the product MA). Multiplying out and grouping the pairs (d,m) with $dm=n$,

$$MA=\sum_{d\le D}\sum_{m\le N}\lambda_d b_m\,(dm)^{-s_*}=\sum_{n\le DN}c_n\,n^{-s_*},\qquad c_n=\sum_{\substack{dm=n\\ d\le D,\ m\le N}}\lambda_d b_m.$$

The only pair with $dm=1$ is $d=m=1$, so $c_1=\lambda_1 b_1=1$. Since $|n^{-s_*}|=n^{-\sigma}$, the triangle inequality gives $|MA|\ge 1-\sum_{n\ge 2}|c_n|n^{-\sigma}$.

Step 3 (the conjugate of B). Since m^y and b_m are real,

$$\bar B=\sum_{m\le N}m^y b_m\,\overline{m^{-\overline{s_*}-\kappa}}=\sum_{m\le N}m^y b_m\,m^{-s_*-\bar\kappa},\qquad |\bar B|=|B|.$$

Step 4 (the product $M\bar B$). For $n=dm$ we have $m^y=n^y d^{-y}$, $m^{-s_*}=n^{-s_*}d^{s_*}$ and $m^{-\bar\kappa}=n^{-\bar\kappa}d^{\bar\kappa}$, hence $d^{-s_*}m^{y-s_*-\bar\kappa}=n^{y-s_*-\bar\kappa}\,d^{-y}d^{\bar\kappa}$. Therefore

$$M\bar B=\sum_{d\le D}\sum_{m\le N}\lambda_d b_m\,d^{-s_*}m^{y-s_*-\bar\kappa}=\sum_{n\le DN}n^{y-s_*-\bar\kappa}\,\beta_n,\qquad \beta_n=\sum_{\substack{dm=n\\ d\le D,\ m\le N}}\lambda_d\,d^{-y}\,d^{\bar\kappa}\,b_m.$$

Step 5 (removing $d^{\bar\kappa}$). Write $d^{\bar\kappa}=1+(d^{\bar\kappa}-1)$. By $|e^w-1|\le e^{|w|}-1$ with $w=\bar\kappa\log d$, $|d^{\bar\kappa}-1|\le d^{|\kappa|}-1\le D^{|\kappa|}-1$. Hence $|\beta_n|\le|c_n'(y)|+\epsilon_n$, with c_n' and ϵ_n as in the statement.

Step 6 (the size of $M\bar B$). Since $|n^{y-s_*-\bar\kappa}|=n^{y-\sigma-\operatorname{Re}\kappa}\le n^{y-\sigma+|\kappa|}$, Steps 4 and 5 give $|M\bar B|\le\sum_n(|c_n'(y)|+\epsilon_n)\,n^{y-\sigma+|\kappa|}$.

Step 7 (conclusion). From $|M||B|=|M||\bar B|=|M\bar B|$ and $|M||A|=|MA|$,

$$|M|\big(|A|-|\gamma||B|\big)=|MA|-|\gamma|\,|M\bar B|\ge 1-\sum_{n\ge 2}|c_n|n^{-\sigma}-|\gamma|\sum_n\big(|c_n'(y)|+\epsilon_n\big)n^{y-\sigma+|\kappa|}=\mathcal{L}.$$

If $\mathcal{L}>0$, the left side is positive, so $M\ne 0$ and $|A|-|\gamma||B|\ge\mathcal{L}/|M|\ge\mathcal{L}/M^+$. Finally $|f_t|=|A+\gamma B|\ge|A|-|\gamma||B|$. □

Remark 4. (i) Nothing in the proof uses that the λ_d are optimal, or even real; only $\lambda_1=1$ is needed. (ii) $\mathcal{L}$ is non-increasing in $|\gamma|$ and in $|\kappa|$ and non-decreasing in σ, and M^+ is non-increasing in σ. Hence the lemma remains true if σ is replaced by any lower bound and $|\gamma|,|\kappa|$ by any upper bounds; the certificate uses the bounds (1). (iii) The algebra of Steps 2–7 was also checked numerically at exact values of s_*,κ,γ computed from the definitions of [Pm, (16)–(18)] (ancillary script `audit_lemmas.py`).

The Euler mollifier $\prod_{p\le P}(1-b_p p^{-s_*})$ of [Pm, Sect. 8.5] is the case $\lambda_d=\prod_{p\mid d}(-b_p)$ for $d\mid\prod_{p\le P}p$, and $\lambda_d=0$ otherwise. Since $\mathcal{L}$ is a concave, piecewise-linear function of $(\lambda_2,\dots,\lambda_D)$, maximising it is an ℓ^1 regression problem. We solve it by iteratively reweighted least squares at the point $x=6\cdot 10^{12}$, $y=y_0$, $t=t_0$. Only the evaluation of $\mathcal{L}$ has to be certified, not the optimisation.

Remark 5. On primes the optimised weights are close to the Euler values $\lambda_p=-b_p$ (for instance $\lambda_{227}=-3.03$, $b_{227}=3.11$), but they use every prime up to D. On squarefree composites they are smaller than the Euler values $\prod_{p\mid d}(-b_p)$ ($\lambda_{30}=-0.86$ against -1.18, $\lambda_{210}=0.55$ against 1.36). On prime powers, where the Euler mollifier has 0, they are moderate ($\lambda_{169}=-1.09$, $\lambda_{121}=-0.87$, $\lambda_{125}=-0.51$, $\lambda_{49}=-0.45$), and on the other non-squarefree d they are small (median $|\lambda_d|=0.03$, maximum 0.34). Doubling D from 60 to 120 raised $\mathcal{L}$ by 0.04 at $t_0=0.157$; with $D=240$, $t_0=0.150$ ($\Lambda=0.17$) stays below -0.13.

mollifier	$t_0 = 0.157$ ($\Lambda = 0.177$)	$t_0 = 0.155$ ($\Lambda = 0.175$)	$t_0 = 0.153$ ($\Lambda = 0.173$)
none (triangle ineq.)	-1.66	-1.79	–
Euler, $p \le 13$ (64 terms)	-0.048	-0.124	–
optimised, $d \le 30$	$+0.030$	–	–
optimised, $d \le 60$	$+0.081$	–	–
optimised, $d \le 120$	$+0.122$	$+0.051$	-0.027
optimised, $d \le 240$	–	–	$+0.0009$
optimised, $d \le 240$, $t_0 = 0.154$ ($\Lambda = 0.174$): $\mathcal{L} = +0.040$			

Table 2: The lower bound $\mathcal{L}$ at $x = 6 \cdot 10^{12}$, $y = 0.2$ (floating point; – = not computed). The Euler row uses Polymath's coefficients $\prod_{p|d}(-b_p)$. Each optimised entry uses weights optimised at that t_0; the ancillary files contain only the weights for $d \le 120$, $t_0 = 0.155$ (`lam_L0175.npy`) and for $d \le 240$, $t_0 = 0.154$ (`lam_L0174.npy`). With the latter, $\mathcal{L} = 8 \cdot 10^{-5}$ at $t_0 = 0.153$, instead of the 0.0009 of weights re-optimised there.

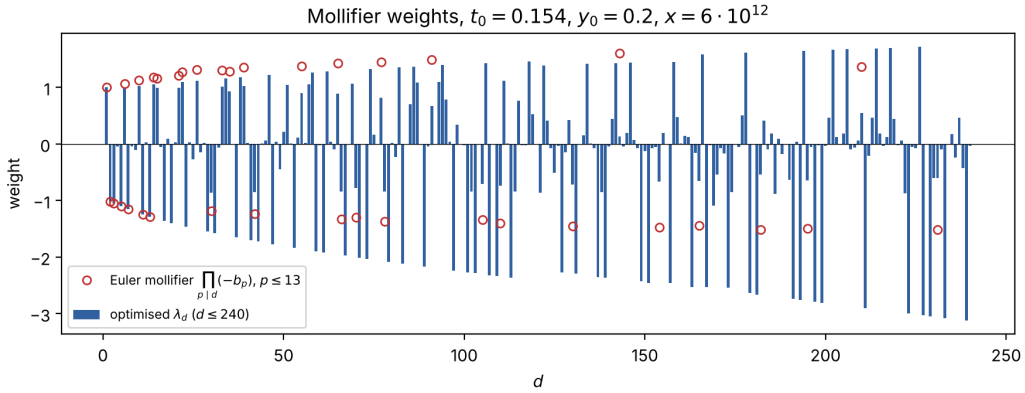


Figure 1: Optimised weights ($t_0 = 0.154$, $d \le 240$) compared with Polymath's Euler mollifier on the primes up to 13, whose coefficients are $\prod_{p|d}(-b_p)$. The optimised mollifier uses every prime up to 240, with $\lambda_p \approx -b_p$, damps the squarefree composite terms, and gives some weight to prime powers (script `weights_fig.py`).

4 Hypothesis (ii): all $x \ge X$ and all y

Throughout this section $t = t_0$ is fixed and $[y_a, y_b] \subset [y_0, \sqrt{1 - 2t_0}]$ is one of the y-intervals of the certificate. The coefficients c_n and $c_n'(y)$ depend on x only through the truncation N (and ϵ_n also through κ), which is a step function. For the bookkeeping we use the slightly larger truncation $N(x) := \lfloor \sqrt{x/4\pi} + \frac{t}{16} \rfloor$, for which $N(x) \ge m$ exactly when $x \ge x_m := 4\pi(m - \frac{t}{16})^2$. Since $\sqrt{a} \le \sqrt{a + \frac{t}{16}} \le \sqrt{a} + \frac{t}{16}$ for $a \ge 1$ and $\frac{t}{16} < 1$, Polymath's truncation satisfies $N(x) - 1 \le N_{\mathrm{Pm}}(x) \le N(x)$; Lemma 6(a) is therefore stated for every truncation between N_a and $N(x)$, and Remark 7 shows that this covers f_t. For an integer $N' \ge 1$ we write $f_t^{(N')}$ for the expression defining f_t with N replaced by N', so that $f_t = f_t^{(N_{\mathrm{Pm}}(x))}$. We write the bounds (1) as functions,

$$\sigma_-(x,y) = \tfrac{1+y}{2} + \tfrac{t}{4}\log\tfrac{x}{4\pi} - \tfrac{t}{x^2}, \qquad \gamma_+(x,y) = e^{0.02y}\big(\tfrac{x}{4\pi}\big)^{-y/2}, \qquad \kappa_+(x,y) = \tfrac{ty}{2(x-6)},$$

and put $\sigma_a(x) = \sigma_-(x, y_a)$, $g_a(x) = \gamma_+(x, y_a)$, $k(x) = \kappa_+(x, y_b)$ and $e(x) = \max_{y\in\{y_a,y_b\}} \big(y - \sigma_-(x, y) + \kappa_+(x, y)\big)$. For $x \geq 200$ and $y_a \leq y \leq y_b$ we have

$$\sigma_-(x, y) \geq \sigma_a(x), \quad \gamma_+(x, y) \leq g_a(x), \quad \kappa_+(x, y) \leq k(x), \quad y - \sigma_-(x, y) + \kappa_+(x, y) \leq e(x), \quad (2)$$

because σ_- and κ_+ increase in y, $\gamma_+(x, y) = \exp\big(y(0.02 - \frac{1}{2}\log\frac{x}{4\pi})\big)$ decreases in y, and $y - \sigma_- + \kappa_+$ is affine in y. Moreover σ_a increases with x, while g_a, k and e decrease. For a truncation N' let $c_n^{(N')}$, $c_n'^{(N')}$ be the coefficients of Lemma 3 with $m \leq N'$, and define

$$\mathcal{L}_{N'}(x) = 1 - \sum_{n\geq 2} \big|c_n^{(N')}\big| n^{-\sigma_a(x)} - g_a(x) \sum_n \Big(\big|c_n'^{(N')}(y_a)\big| + \eta_n^{(N')}(x)\Big) n^{e(x)},$$

$$\eta_n^{(N')}(x) = \sum_{\substack{dm=n \\ d\leq D,\ m\leq N'}} |\lambda_d|\, b_m \Big(d^{-y_a} - d^{-y_b} + d^{-y_a}\big(D^{k(x)} - 1\big)\Big), \qquad M^+(x) = \sum_{d\leq D} |\lambda_d| d^{-\sigma_a(x)},$$

and, for real $v \geq 2$, with $x_v = 4\pi(v - \frac{t}{16})^2$ and $b_v = e^{\frac{t}{4}\log^2 v}$,

$$F(v) = b_v\, v^{-\sigma_a(x_v)} \sum_{d\leq D} |\lambda_d| d^{-\sigma_a(x_v)} + g_a(x_v)\, D^{k(x_v)}\, b_v\, v^{e(x_v)} \sum_{d\leq D} |\lambda_d| d^{e(x_v)-y_a}.$$

$F(m)$ bounds the contribution of all the new pairs (d, m), $d \leq D$, that appear when N reaches m.

Lemma 6. *Let $x_a \geq 200$ and $N_a = N(x_a)$.*

(a) For every $x \geq x_a$, every $y \in [y_a, y_b]$ and every integer N' with $N_a \leq N' \leq N(x)$,

$$\big|f_t^{(N')}(x + iy)\big| \;\geq\; \frac{\mathcal{L}_{N_a}(x_a) - \sum_{N_a<m\leq N'} F(m)}{M^+(x_a)} \;\geq\; \frac{\mathcal{L}_{N_a}(x_a) - \sum_{N_a<m\leq N(x)} F(m)}{M^+(x_a)}$$

the first inequality holding whenever its right-hand side is positive.

(b) F is strictly decreasing on $[2, \infty)$. Consequently, for integers $N_a + 1 = a_0 < a_1 < \cdots < a_K = N_b + 1$, $\sum_{N_a<m\leq N_b} F(m) \leq \sum_{k<K}(a_{k+1} - a_k)F(a_k)$, and $\sum_{m>N_a} F(m) \leq \int_{N_a}^{\infty} F(v)\, dv$.

Proof. (a) Fix $x \geq x_a$, $y \in [y_a, y_b]$ and $N_a \leq N' \leq N(x)$, and write N for N' in this proof. The second inequality holds because $F \geq 0$. By (1) and (2), $\sigma = \operatorname{Re} s_* \geq \sigma_a(x)$, $|\gamma| \leq g_a(x)$, $|\kappa| \leq k(x)$ and $y - \sigma + |\kappa| \leq e(x)$. By Lemma 3 and Remark 4(ii),

$$M^+(x)\,\big|f_t^{(N)}(x + iy)\big| \;\geq\; 1 - \sum_{n\geq 2} \big|c_n^{(N)}\big| n^{-\sigma_a(x)} - g_a(x) \sum_n \Big(\big|c_n'^{(N)}(y)\big| + \epsilon_n^{(N)}\Big) n^{e(x)},$$

where $\epsilon_n^{(N)}$ is formed with $D^{k(x)} - 1 \geq D^{|\kappa|} - 1$; here we used that $u \mapsto n^u$ is non-decreasing for $n \geq 1$. Split every coefficient into the pairs (d, m) with $m \leq N_a$ and the new pairs with $N_a < m \leq N$. For the old pairs, $d^{-y} \leq d^{-y_a}$ and $\big|c_n'^{(N_a)}(y)\big| \leq \big|c_n'^{(N_a)}(y_a)\big| + \sum_{dm=n,\, m\leq N_a} |\lambda_d| b_m (d^{-y_a} - d^{-y_b})$, so the old pairs contribute at most what they contribute to $\mathcal{L}_{N_a}(x)$. For the new pairs, the triangle inequality bounds their contribution by

$$\sum_{N_a<m\leq N} \sum_{d\leq D} |\lambda_d|\, b_m \Big((dm)^{-\sigma_a(x)} + g_a(x) D^{k(x)} d^{-y_a} (dm)^{e(x)}\Big) \;\leq\; \sum_{N_a<m\leq N} F(m),$$

since $m \le N' \le N(x)$ means $x \ge x_m$, so that $\sigma_a(x) \ge \sigma_a(x_m)$, $g_a(x) \le g_a(x_m)$, $k(x) \le k(x_m)$ and $e(x) \le e(x_m)$, and $d^{-y_a}(dm)^e = m^e d^{e-y_a}$. Finally $\mathcal{L}_{N_a}(x) \ge \mathcal{L}_{N_a}(x_a)$ and $M^+(x) \le M^+(x_a)$ by the same monotonicity in x.

(b) Write $L = \log v$, $\ell = \log(v - \frac{t}{16})$, so that $\log \frac{x_v}{4\pi} = 2\ell$, and note $x_v \ge x_2 > 48$ for $v \ge 2$. Then

$$\sigma_a(x_v) = \tfrac{1+y_a}{2} + \tfrac{t}{2}\ell - \tfrac{t}{x_v^2} > 0, \qquad \frac{d}{dv}\sigma_a(x_v) = \frac{t/2}{v - t/16} + \frac{2t\,x_v'}{x_v^3} \;\ge\; \frac{t/2}{v - t/16},$$

and, for $y \in \{y_a, y_b\}$, $e_y(v) := y - \sigma_-(x_v, y) + \kappa_+(x_v, y) = \frac{y-1}{2} - \frac{t}{2}\ell + \frac{t}{x_v^2} + \frac{ty}{2(x_v - 6)}$ satisfies $e_y'(v) \le -\frac{t/2}{v - t/16}$ and $e_y(v) \le \frac{y_b - 1}{2} + \frac{t}{48^2} + \frac{t}{84} < 0$, since $y_b \le 0.832$ and $t < 0.16$.

First term. It is $T_1(v) = e^{\varphi_1(v)} S_1(\sigma_a(x_v))$ with $\varphi_1 = \frac{t}{4}L^2 - \sigma_a(x_v)L$ and $S_1(\sigma) = \sum |\lambda_d| d^{-\sigma}$, which is non-increasing in σ, so $S_1(\sigma_a(x_v))$ is non-increasing in v. Since $L \ge 0$,

$$\varphi_1'(v) = \frac{t}{2}\frac{L}{v} - \frac{d\sigma_a(x_v)}{dv}L - \frac{\sigma_a(x_v)}{v} \;\le\; \frac{t}{2}L\Big(\frac{1}{v} - \frac{1}{v - t/16}\Big) - \frac{\sigma_a(x_v)}{v} < 0.$$

Second term. Since v^e and $S_2(e) = \sum |\lambda_d| d^{e-y_a}$ are non-decreasing in e, the second term equals $T_2(v) = \max_{y \in \{y_a, y_b\}} g_a(x_v) D^{k(x_v)} e^{\psi_y(v)} S_2(e_y(v))$ with $\psi_y = \frac{t}{4}L^2 + e_y(v)L$. Here $g_a(x_v) = e^{0.02 y_a}(v - \frac{t}{16})^{-y_a}$ and $D^{k(x_v)}$ decrease, $S_2(e_y(v))$ does not increase, and

$$\psi_y'(v) = \frac{t}{2}\frac{L}{v} + e_y'(v)L + \frac{e_y(v)}{v} \;\le\; \frac{t}{2}L\Big(\frac{1}{v} - \frac{1}{v - t/16}\Big) + \frac{e_y(v)}{v} < 0.$$

A maximum of two decreasing functions is decreasing, so T_2 decreases, and $F = T_1 + T_2$ is strictly decreasing. For a decreasing F, $F(m) \le F(a_k)$ for $a_k \le m < a_{k+1}$, and $F(m) \le \int_{m-1}^{m} F$, which gives the two consequences. □

Remark 7 (Polymath's truncation). The function f_t of [Pm, Thm. 1.3] is $f_t^{(N_{\mathrm{Pm}}(x))}$ with $N(x) - 1 \le N_{\mathrm{Pm}}(x) \le N(x)$. The certificate consists of consecutive chunks: chunk j starts at $x_a = x_{N_a}$ (the first one at $X + \sqrt{1 - y_0^2}$) and certifies that the numerator of Lemma 6(a) is positive with the sum extended to $m \le N_b$, where $N_b + 1$ is the N_a of chunk $j + 1$ (the last chunk extends the sum to infinity, Lemma 8). Let x lie in the x-range of chunk j. If $N_{\mathrm{Pm}}(x) \ge N_a$, Lemma 6(a) applies with $N' = N_{\mathrm{Pm}}(x)$. Otherwise $N_{\mathrm{Pm}}(x) = N_a - 1$; for $j \ge 2$ this is the largest truncation of chunk $j - 1$, and Lemma 6(a) for that chunk applies, since it holds for every x above its starting point; for $j = 1$ this does not occur, because $\sqrt{X/4\pi} = 690891.17$ gives $N_{\mathrm{Pm}}(x) \ge 690891 = N_a$ for all $x \ge X$. The certified majorant of the error terms $e_A + e_B + e_{C,0}$ is valid for both truncations (its sums run over $n \le N_{\mathrm{Pm}} \le N(x)$, and $N_{\mathrm{Pm}} \ge 690891$ in $e_{C,0}$). On the barrier $[X, X + 1]$ both truncations equal 690891.

Lemma 8 (the infinite tail)**.** *Let $V = e^{60}$. For $v \ge V$, $F(v) \le F(V)V^2 v^{-2}$. Hence, if $F(V)V^2 < 1$ and $N_a = v_0 < v_1 < \cdots < v_J$ with $v_J \ge V$, then $\sum_{m > N_a} F(m) \le \sum_{j<J}(v_{j+1} - v_j)F(v_j) + e^{-60}$.*

Proof. With the notation of the previous proof, $v\varphi_1'(v) \le -\sigma_a(x_v) \le -\frac{t}{2}\ell + \frac{t}{x_v^2}$ and $v\psi_y'(v) \le e_y(v) \le -\frac{t}{2}\ell + 10^{-6}$ for $v \ge V$; the other factors of T_1 and T_2 do not increase. Therefore $v\frac{d}{dv}\log(v^2 T_i) \le 2 - \frac{t}{2}\ell + 10^{-6} < 0$, because $\frac{t}{2}\ell \ge \frac{0.15399}{2} \cdot 59.99 > 4.6$. So $v^2 F(v)$ is non-increasing on $[V, \infty)$, and $\int_V^\infty F \le F(V)V^2 \int_V^\infty v^{-2} dv < V^{-1}$. On $[N_a, v_J]$ we use Lemma 6(b). (In the script the loop stops when the upper end of the Arb ball for $\log v_J$ reaches 60, so v_J may fall short of V by a relative amount below 10^{-24}, the radius of that ball. The missing piece $\int_{v_J}^{V} F \le (V - v_J)F(v_{J-1})$ is then less than 10^{-21} times the last term $(v_J - v_{J-1})F(v_{J-1})$ of the sum, far below the relative slack $\ge 10^{-13}$ that the outward-rounded summation adds to it.) □

We cover $x \geq X + \sqrt{1-y_0^2}$ by chunks $[x_{N_a}, x_{N_b+1})$ (the first one starts at $x_a = X + \sqrt{1-y_0^2}$). On each chunk Lemma 6 gives $|f_{t_0}| \geq (\mathcal{L}_{N_a}(x_a) - \sum_{N_a<m\leq N_b} F(m))/M^+(x_a)$, with the sum bounded by blocks of ratio $1 + 2^{-9}$. Once $\mathcal{L}_{N_a}(x_a)$ exceeds the bound of Lemma 8 (computed with $v_{j+1} = 1.01v_j$), the last chunk is infinite. The y-range $[0.2, \sqrt{1-2t_0}] = [0.2, 0.8319]$ is cut into 7 intervals. In the Arb run, near y_0, ten finite chunks reach $x \approx 5.3 \cdot 10^{13}$, and the eleventh chunk, from there on, is the infinite one. The certified lower bound for $|f_{t_0}|$ on the whole region is 0.00594, against $e_A + e_B + e_{C,0} \leq 2.98 \cdot 10^{-7}$ (Table 3). All the steps are listed in Appendix A.

5 Hypothesis (iii): the barrier

On $X \leq x \leq X + 1$ and $0 \leq t \leq t_0$, $N = 690891$ is constant, so f_t is holomorphic. We split $[0, t_0]$ into steps $[t_1, t_2]$ and use the rectangle $R = [X, X+1] \times [\sqrt{y_0^2 + 2(t_0 - t_2)}, 1]$, which contains the region of (iii) for every t in the step. With the derivative bounds D_z, D_t of [Pm, Lemma 8.4] and a mesh $\{z_j\}$ of ∂R with spacing h, the conditions

$$\min_j |f_{t_1}(z_j)| > D_z h, \qquad \min_j |f_{t_1}(z_j)| - \tfrac{D_z h}{2} - D_t(t_2 - t_1) - E > 0, \qquad \text{winding number} = 0,$$

imply by Rouché's theorem that H_t has no zero in R for $t \in (t_1, t_2]$. The time $t = 0$ is covered by (i). The sums are evaluated with Polymath's Taylor scheme [Pm, Sect. 7] on dyadic blocks of n, with the phases $\frac{X_c}{2} \log n \bmod 2\pi$ computed to 128 bits. At $t = 0$ the barrier only needs $y \geq \sqrt{y_0^2 + 2t_0} \approx 0.59$, where $|f_0| \geq 4.79$. In the Arb run, 73 time steps and 39 840 evaluations suffice, with $\min |f_t| \geq 1.60$ on all meshes and minimal margin 0.3459. The last step ends at a floating-point number $\geq t_0$, and the winding numbers are certified with interval arithmetic.

6 Numerical certification

Two implementations were used. (a) A double-precision implementation with an explicit a priori error budget, used to design the computation; it gives slightly larger margins than (b), since it bounds less conservatively. (b) The certificate scripts `cert_region_ii.py` and `cert_barrier.py` (ancillary files). They compute every transcendental quantity with Arb [Arb] through python-flint, convert balls to floating-point intervals rounded outward by one ulp, and perform the large sums (up to about $5 \cdot 10^8$ terms) using only $+, -, \times$ with outward rounding and Higham's bound for sums. To keep the number of Arb calls moderate, monotone factors such as $n^{-\sigma}$ are bounded by their values at the left ends of short geometric blocks of n (ratio $1 + 2^{-13}$ in (ii), $1 + 2^{-10}$ for the derivative bounds of (iii)). The only libm call in a certifying step is the argument function in the winding-number check, covered by a slack of 10^{-6} per term. The scripts stop with an error whenever a check fails, so they cannot report a certificate by mistake. The results of the Arb run (python-flint, Python 3.13) are summarised in Table 3; the complete logs are among the ancillary files.

The Taylor evaluation of f_t was checked against direct summation (agreement to 10^{-15}), and a separate float evaluator agrees to the precision of its phases. Code reviews against [Pm] raised three points (rounding directions, a rigorous winding-number check, the end point of the time range); these are fixed in the version used for Table 3. Appendix A lists every step of the certification, with the function of the scripts that carries it out. Appendix B gives the SHA-256 hashes of the inputs and a second run of the same scripts on a different platform, which reproduces Table 3.

Proof of Theorem 1. Take $t_0 = 0.15399$, $y_0 = 0.2$, $X = 5\,998\,313\,329\,980.3135$ in Theorem 2. Hypothesis (i) holds because $X/2 < 3 \cdot 10^{12}$ [PT]. Hypothesis (ii) follows from Lemmas 3, 6 and 8,

hypothesis (ii): y-interval	chunks	certified $\lvert f_{t_0}\rvert \geq$
$[0.200, 0.205]$	11	0.00594
$[0.205, 0.215]$	9	0.00966
$[0.215, 0.235]$	7	0.01931
$[0.235, 0.275]$	5	0.02836
$[0.275, 0.355]$	3	0.01803
$[0.355, 0.515]$	2	0.01855
$[0.515, 0.831877]$	2	0.14245
$e_A + e_B + e_{C,0} \leq 2.98 \cdot 10^{-7}$ for all $x \geq X + \sqrt{1-y_0^2}$		
hypothesis (iii)	73 steps, 39 840 evaluations, margin ≥ 0.345	

Table 3: The Arb certificate for $t_0 = 0.15399$, $y_0 = 0.2$, $X = 5\,998\,313\,329\,980.3135$, $D = 240$ (python-flint 0.9.0, Python 3.13, Windows 11; total time about one hour on a laptop).

Corollary 1.4 of [Pm] and the certified bounds of Table 3, since $0.00594 > 2.98 \cdot 10^{-7}$. Hypothesis (iii) follows from Section 5 and the barrier certificate. Hence $\Lambda \leq t_0 + \frac{1}{2}y_0^2 = 0.17399$. □

7 A by-product: counting the zeros of H_{t_0}

The certificate of hypothesis (ii) gives more than the absence of zeros: it also counts the zeros of H_{t_0} below the line $y = y_0$, with a uniformly bounded error. Write $\theta(x)$ for a continuous branch of $\arg B_{t_0}(x + iy_0)$, where $B_t(x+iy) = M_t(\frac{1+y-ix}{2})$ as in [Pm]; then $\theta'(x) = -\frac{1}{2}\operatorname{Re}\big(\alpha + \frac{t_0}{2}\alpha\alpha'\big)(\frac{1+y_0-ix}{2}) = -\frac{1}{4}\log\frac{x}{4\pi} + O(\frac{1}{x})$.

Proposition 9. *Let t_0, y_0, X be as in Theorem 1 and $X + \sqrt{1-y_0^2} \leq a < b$. For every zero $z_k = x_k + iy_k$ of H_{t_0} put $h_k = y_0 - y_k$ and*

$$w_k = \frac{1}{\pi}\Big(\arctan\frac{b-x_k}{h_k} - \arctan\frac{a-x_k}{h_k}\Big) \in (0,1).$$

Then $0 < h_k < 2y_0$ for all k, and

$$\Big|\sum_k w_k - \frac{\theta(a)-\theta(b)}{\pi}\Big| < 3.001.$$

Consequently, for every $R > \frac{4y_0}{\pi}$, the number of zeros of H_{t_0} (with multiplicity) with $a+R \leq x_k \leq b-R$ is at most $\big(\frac{\theta(a)-\theta(b)}{\pi} + 3.001\big)\big/\big(1 - \frac{4y_0}{\pi R}\big)$.

Proof. By Theorem 1 (more precisely, by Proposition 3.3 of [Pm] applied with our certificates), H_{t_0} has no zeros with $y_k \geq y_0$, and by symmetry none with $y_k \leq -y_0$; hence $0 < h_k < 2y_0$. Since H_{t_0} is even, entire of order 1 and positive at 0, the Hadamard product gives, with $\pm k$ grouped,

$$\frac{d}{dx}\arg H_{t_0}(x+iy_0) = \sum_k \operatorname{Im}\frac{1}{x+iy_0-z_k} = -\sum_k \frac{h_k}{(x-x_k)^2+h_k^2},$$

so $\arg H_{t_0}(a+iy_0) - \arg H_{t_0}(b+iy_0) = \pi\sum_k w_k$ (termwise integration is justified by dominated convergence). On the other hand, on the segment $[a,b]+iy_0$ the certificate gives, at every point,

$|MA-1| \le \sum_{n\ge 2}|c_n|n^{-\sigma} < 1$, $|M-1| \le \sum_{2\le d\le D}|\lambda_d|d^{-\sigma} < 1$ (Table 5: $M^+ \le 1.97$) and $|\gamma B| < |A|$ (Lemma 3). Hence $f_{t_0} = \frac{MA}{M}\big(1+\frac{\gamma B}{A}\big)$ is a product of three factors whose real parts are positive or reciprocal of positive, so at every point of the segment the sum of the principal arguments of the three factors lies in $(-\frac{3\pi}{2}, \frac{3\pi}{2})$. The function f_{t_0} jumps where N increases, but $H_{t_0}/B_{t_0} = f_{t_0} + E$ is continuous, with $|E| \le 3\cdot 10^{-7}$ and $|f_{t_0}| \ge 0.0059$, so $\arg(f_{t_0}+E)$ differs from $\arg f_{t_0}$ by less than 10^{-4} modulo 2π. On each interval of x where N is constant, $\phi(x) = \mathrm{Arg}(MA) - \mathrm{Arg}(M) + \mathrm{Arg}(1+\frac{\gamma B}{A})$ is a continuous branch of $\arg f_{t_0}$ with values in $(-\frac{3\pi}{2}, \frac{3\pi}{2})$, because each of the three factors stays in the open right half-plane. At a point where N increases to m, M is continuous and A changes by its new term, of modulus at most $3\cdot 10^{-7}$ for $m \ge 690892$, while $|MA| \ge 0.0117$; so $\mathrm{Arg}(MA)$ jumps by less than 10^{-4}, $\mathrm{Arg}(M)$ does not jump, and $\mathrm{Arg}(1+\frac{\gamma B}{A})$ jumps by less than π. Since f_{t_0} changes by at most $2|E| \le 6\cdot 10^{-7}$ (both one-sided limits approximate the continuous function H_{t_0}/B_{t_0}), the jump of ϕ is within $1.1\cdot 10^{-4}$ of a multiple of 2π and smaller than $\pi + 10^{-4}$; hence it is less than 10^{-3}, and no multiple of 2π is gained or lost. Hence the continuous branch of $\arg(H_{t_0}/B_{t_0})$ that agrees with $\phi + 2\pi k$ up to 10^{-4} at $x = a$ does so, with the same integer k, on the whole segment, and its values at a and b differ by less than $3\pi + 2\cdot 10^{-3}$ (the integer k is the same at both ends, so the jumps are not added up). Combining, $|\pi\sum_k w_k - (\theta(a)-\theta(b))| < 3\pi + 2\cdot 10^{-3}$. For the last claim, a zero with $a + R \le x_k \le b - R$ has $w_k \ge 1 - \frac{2}{\pi}\arctan\frac{h_k}{R} \ge 1 - \frac{4y_0}{\pi R}$. □

Since $(\theta(a)-\theta(b))/\pi = \frac{1}{4\pi}\int_a^b \log\frac{x}{4\pi}\,dx + O(\frac{b-a}{a})$, the Poisson-smoothed number of zeros of H_{t_0} in any window above X is given by the main term of the Riemann–von Mangoldt formula with an error of at most $3.001 + O(\frac{b-a}{a})$. For comparison, explicit bounds for $S(T)$ give an error growing like a constant times $\log T$ for ζ; the function H_{t_0} with $t_0 > 0$ is smoother than H_0, so the comparison is only indicative.

8 Ideas that do not improve the bound

We record three natural ideas that we tested and that do not lower Λ at this height, because they explain where the limit of the method lies, and then some smaller levers.

Attraction by the other zeros. De Bruijn's bound $\Lambda \le t_0 + \frac{1}{2}y_0^2$ uses only the attraction between a zero of largest imaginary part and its conjugate. By Proposition 3.1 of [Pm], every other zero of H_t also pulls it towards the real axis, with a contribution at least $2y/(\Delta^2+4y^2)$ for a zero at horizontal distance Δ. On average this would roughly halve the time $\frac{1}{2}y_0^2$. A rigorous bound, however, must allow the worst admissible placement of the zeros. Proposition 9 gives a Poisson-weighted count $\sum_k w_k \ge \rho L - 3.001$ (with $\rho = \frac{1}{4\pi}\log\frac{X}{4\pi} \approx 2.1$) for every window of length L. In the worst placement compatible with this, our estimate gives only $\frac{dy}{dt} \le -\frac{1}{y} - 1.9\,y$, and a descent time $\frac{1}{3.8}\log(1+1.9y_0^2) = 0.0193$ instead of 0.0200. The gain is below 10^{-3}.

The heat flow as an average of Euler products. Since $e^{\frac{t}{4}L^2} = \mathbb{E}\,e^{cZL}$ for a standard Gaussian Z and $c = \sqrt{t/2}$, the main sum of f_t is

$$\sum_{n\le N} b_n n^{-s_*} = \mathbb{E}_Z\Big[\sum_{n\le N} n^{-(s_*-cZ)}\Big],$$

a Gaussian average, in the real direction, of shifted partial sums of ζ, centred at $\mathrm{Re}\,s_* \approx \frac{1+y}{2} + \frac{t}{4}\log\frac{x}{4\pi} > 1$ with width c. Where the shift lands in $\sigma' > 1.15$, the partial sum equals the

Euler product up to a negligible tail. There, for every choice of the phases p^{-iT} simultaneously, $\operatorname{Re}\zeta(\sigma'+iT) \geq \frac{\zeta(2\sigma')}{\zeta(\sigma')}\cos\Phi(\sigma')$ with $\Phi(\sigma)=\sum_p \arcsin p^{-\sigma} < \frac{\pi}{2}$. This handles all phases at once, which a mollified triangle inequality cannot do. The part of the Gaussian below $\sigma' \approx 1$ is not controlled, however. At $X = 6\cdot 10^{12}$, $y_0 = 0.2$, $t = 0.154$, the resulting lower bound is -1.28, against $+0.040$ for the optimised mollifier. The identity is still instructive. It shows why the optimised weights on primes are close to the Euler factors, $\lambda_p \approx -b_p$ (Remark 5). It also suggests why t_0 behaves like $C/\log X$: the Gaussian is centred at $\frac{1+y}{2} + \frac{t}{4}\log\frac{x}{4\pi}$, which must stay a fixed distance above 1 for the uncontrolled mass to be small, while its width $\sqrt{t/2}$ tends to 0.

The trace of the zeros in the primes. The previous two ideas work on the side of ζ. The explicit formula offers a global alternative on the side of the primes. Write $u = \log x$ and $E(u) = e^{-u/2}\big(\psi(e^u) - e^u\big)$, so that $E(u) \approx -\sum_\rho e^{(\beta-\frac12)u}e^{i\gamma u}/\rho$. The component of E at the frequency γ of one zero describes an orbit whose amplitude grows like $e^{(\beta-\frac12)u}$. For ζ the orbit of the first zero is a closed ellipse of constant amplitude (Figure 2(a)). A useful control is the Davenport–Heilbronn function $f(s) = \frac12(1-i\kappa_0)L(s,\chi) + \frac12(1+i\kappa_0)L(s,\bar\chi)$, with χ a complex character modulo 5. It satisfies a functional equation of the same type but has no Euler product, and it has zeros off the critical line [DH, BS]. Its orbits are stable for zeros on the line (b) and open into a spiral for the zero $0.8085 + 85.699i$ (c). The measured growth rate agrees with $\beta - \frac12 = 0.3085$ (d). For f, E is defined with $\psi_f(x) = \sum_{n\leq x}\Lambda_f(n)$, where $-f'/f = \sum \Lambda_f(n)n^{-s}$, and no main term, since f is entire. An independent recomputation from $\Lambda_f(n)$, $n \leq 3\cdot 10^7$, with a Gaussian window of width 1 in u, gives the slope 0.308.

This is the right kind of object for detecting zeros that have not been computed, since it uses only the primes. It does not, however, help with Λ, for two quantitative reasons. First, to isolate a zero at height $\gamma \geq X$ one needs ψ sampled with step about $1/\gamma$ in $\log x$, with $x \gg \gamma$, over a range of u longer than $\log\gamma$. At $\gamma \approx 3\cdot 10^{12}$ this means about 10^{14} values of $\psi(x)$ for x up to about 10^{25}, far more than computing the zeros near that height directly. Second, without knowing γ, an off-line zero becomes visible in the aggregate size of E only when $e^{(\beta-\frac12)u}/\gamma$ exceeds the background of the other zeros, which is of order u^2. For $\gamma \geq 3\cdot 10^{12}$ this requires $x \approx 10^{54}$ if $\beta - \frac12 = 0.31$, and $x \approx 10^{370}$ if $\beta - \frac12 = 0.05$. At best the method would extend the verification of RH, that is, increase X, and it would do so at a much higher cost than the standard methods. It gives no information on H_t for $t > 0$ beyond that. The comparison with the Davenport–Heilbronn function shows the difference that the Euler product makes, but only at heights where it can be computed.

Smaller levers. We also tried several smaller changes at $X \approx 6\cdot 10^{12}$. None of them gains enough to be worth a certificate. First, with the weights fixed, $y_0 = 0.2$ is the best of the values 0.15, 0.17, 0.2 and 0.24. Second, inserting the exact phases of the primes $p \leq 13$ at the height X, instead of the worst case over the torus, raises $\mathcal{L}$ by only 0.0018. Third, a hybrid of the mollifier with the Gaussian average of the previous paragraph (a Hubbard–Stratonovich form of the same identity) gives $\mathcal{L} = -1.16$ at $t = 0.154$, against -1.28 for the Gaussian average alone and $+0.040$ for the optimised mollifier. Fourth, the torus cannot be reduced to a few primes. In a principal component analysis of the dependence of f_t on the prime phases, the share of the mass outside the leading k components is 0.99, 0.49, 0.15 and 0.038 for $k = 5$, 50, 1000 and 10^4, so about 10^4 of the $\pi(N) \approx 5.6\cdot 10^4$ phases matter. Finally, we extended the optimised mollifier of length 240 by the Euler values $\lambda_p = -b_p$ on all primes $240 < p \leq P$. Table 4 separates what is certified from what is not. Only the first row enters Theorem 1, and the others are not used anywhere in this paper.

mollifier	$\mathcal{L}$ (floating point; $x = 6 \cdot 10^{12}$, $y = 0.2$, $t = 0.154$)	status	consequence
optimised, $d \le 240$	0.0405	certified for all $x \ge X + \sqrt{1-y_0^2}$ and all y, with $t_0 = 0.15399$ (Table 3)	$\Lambda \le 0.17399$ (Theorem 1)
+ Euler on $240 < p \le 1000$	0.0626	not certified	–
+ Euler on $240 < p \le 3000$	0.0749	not certified	–
joint optimisation, about 1000 weights	not computed	extrapolation	$\Lambda \approx 0.172$ (estimate only)

Table 4: Longer mollifiers. The value 0.0405 is a single floating-point evaluation of $\mathcal{L}$ at one point. For the first row, the same evaluation at $x_a = X + \sqrt{1-y_0^2}$, $y = 0.2$, $t_0 = 0.15399$ gives 0.0400; making it uniform over the first y-interval $[0.2, 0.205]$ as in Lemma 6 lowers it to 0.02195, and outward rounding and block bounds lower it to the certified $\mathcal{L}_{N_a}(x_a) \ge 0.02188$ (ancillary script `audit_lemmas.py` and Table 5).

The gain is about $+0.012$ in $\mathcal{L}$ each time P is tripled. Extrapolating the relation between $\mathcal{L}$ and t_0 of Table 2 gives $\Lambda \approx 0.1732$ for $P = 3000$ and perhaps 0.172 with a joint optimisation of about 1000 weights, that is, about 0.002 below Theorem 1. This is a research prospect, not a result. Certifying it would need the chunking of Section 4 with D about 3000, so that every chunk involves sums with about $DN \approx 2 \cdot 10^9$ terms. The figures of the last three rows are from the author's working notes, and the scripts that produced them are not among the ancillary files.

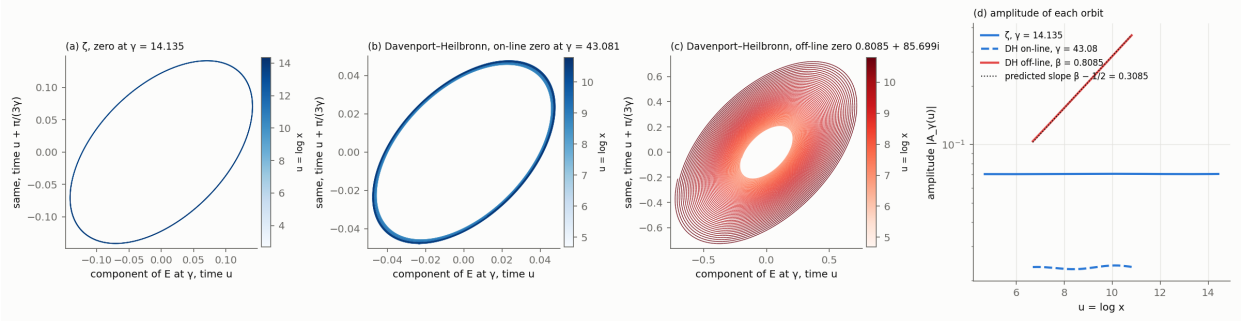


Figure 2: Orbits of the component at frequency γ of the normalised prime error $E(u)$, $u = \log x$, plotted against the same component at the delay $\pi/(3\gamma)$. (a) ζ, $\gamma = 14.135$. (b) Davenport–Heilbronn, on-line zero $\gamma = 43.081$. (c) Davenport–Heilbronn, off-line zero $0.8085 + 85.699i$. (d) Amplitudes, with the predicted slope $\beta - \frac{1}{2}$. Illustration only; no part of the proof depends on this figure.

9 Discussion

The improvement comes entirely from hypothesis (ii); the barrier is easy at this height. Pushing the same method further: with $D \le 240$ and weights re-optimised at $t_0 = 0.153$ ($\Lambda = 0.173$), the bound $\mathcal{L}$ at $x = X$ is still positive, but only by 0.0009, which is too small to cover all $x \ge X$. So,

with the present verification of RH and the weights we found for $D \le 240$, 0.174 is essentially the limit of the method (a numerical observation, not a proven optimality statement); longer mollifiers might gain about 0.002 (Table 4, not certified). A smaller mollifier ($D = 120$, Table 2) is expected to give $\Lambda \le 0.175$ already; this was obtained with an earlier version of the scripts and is not part of the certificate of this paper (only the weights `lam_L0175.npy` are provided). Polymath's heuristic $\Lambda \approx C/\log X$ [Pm, Sect. 10] still applies: our numerical search for the minimum of $|f_{t_0}|$ over the phase torus (not a certified computation) suggests that $\Lambda \approx 0.15$ would be within reach at the same height, so better certified lower bounds for this minimum remain the natural way to push further without new RH verification.

Why the torus, and what it costs. The phase torus is not an arbitrary choice. The main sum depends on x only through the phases $n^{-ix/2}$, and by unique factorisation these are determined by the prime phases $\theta_p = \frac{x}{2}\log p \pmod{2\pi}$. Since the numbers $\log p$ are linearly independent over $\mathbb{Q}$, Kronecker's theorem shows that the curve $x \mapsto (\theta_p)_p$ is dense in the torus, and no proper subtorus or subvariety contains it. If one uses only the multiplicative independence of the primes, the torus is therefore the smallest set that has to be controlled; this is the setting of the mollifier bound of Lemma 3, which holds for all phases at once. The torus is, however, a relaxation of what hypothesis (ii) actually requires. The coefficients of f_t change with x, and the hardest range is $x \in [X, cX]$ for a moderate c: beyond it $\frac{t}{4}\log\frac{x}{4\pi}$ has grown enough for the bound to be comfortable. Over such a finite range the curve is very thin in a torus of dimension $\pi(N) \approx 5.6 \cdot 10^4$. Figure 3 illustrates this on toy examples. With two primes, even a short window of x crosses the region where a small Dirichlet polynomial is close to 0 (a), and a longer range fills the torus (b). In higher dimension (c), the median distance from the curve of a window to a random point of the torus grows quickly with the number of primes, and lengthening the window by a factor 100 reduces it only moderately. Exploiting this thinness would require knowing where the curve lies above X; by the explicit formula, this is information about the zeros of ζ above height X, which is exactly what the verification of RH provides only below X. We see no way around this, and we record the comparison as an explanation of why the bounds depend on X only through $\log X$.

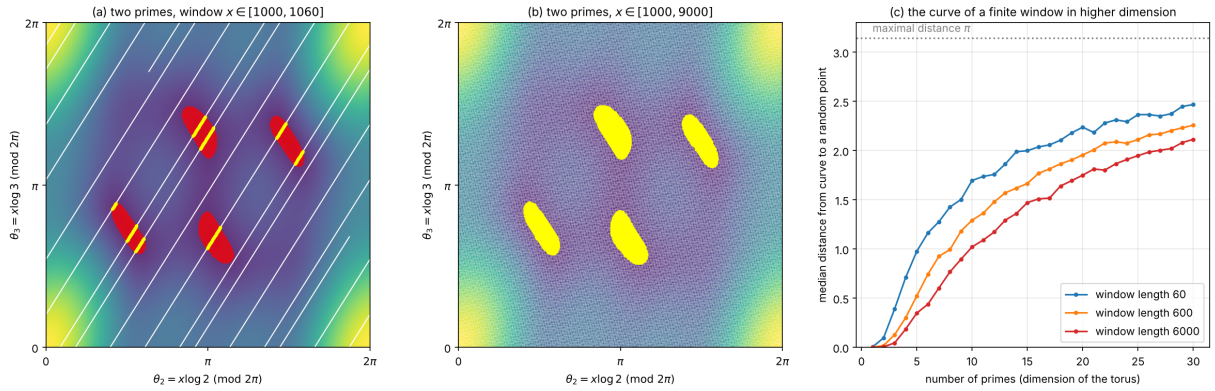


Figure 3: Phase torus versus the actual curve $x \mapsto (x\log p \bmod 2\pi)_p$. (a), (b): the Dirichlet polynomial $\sum n^{-0.55}e^{-i\phi_n}$ over $n \in \{1,2,3,4,6,8,9,12\}$, with $\phi_n = v_2(n)\theta_2 + v_3(n)\theta_3$; red: $|\cdot| < 0.25$; white: the curve; yellow: points of the curve in the red region. (c): median over 40 random target points of the sup-norm distance to the curve for $x \in [10^4, 10^4 + L]$, using the first d primes. Illustration only; no part of the proof depends on this figure.

The constant in the $C/\log X$ law. In Part 34 [CE34] we study how the width of the strip left uncontrolled by hypothesis (ii) depends on t_0 and on the height. Without a mollifier, under the barrier condition, the method gives $\Lambda \le (4w_0 + o(1))/\log X$ with $\zeta(\frac{1}{2} + w_0) = 2$, $4w_0 = 4.915$; and no mollified triangle bound with mollifier length at most $N/2$ can give a constant below 4. In these terms the present bound corresponds to $C = 0.17399 \cdot \log(X/4\pi) = 4.68$.

The torus minimum as a function of the height. The numerical minimum of $|f_t|$ over the phase torus mentioned at the beginning of this section can also be followed in X; this is not covered by [CE34]. We computed it by L-BFGS on all the prime phases (55 874 of them at $X = 6 \cdot 10^{12}$) from several starting points, and bisected in t at $y_0 = 0.2$ for the critical value $t^*(X)$ above which the minimum is positive. We found $t^* \in [0.1525, 0.155]$ at $X = 10^{11}$, $t^* \in [0.135, 0.14]$ at $X = 10^{12}$, and $t^* \le 0.13$ at $X = 6 \cdot 10^{12}$, where the minimum is $+0.394$ at $t = 0.13$ and all 12 starts gave positive values. Thus $t^* \log X \approx 3.9$, 3.8 and at most 3.8. In the normalisation of [CE34], $(t^* + \frac{1}{2}y_0^2)\log(X/4\pi) \approx 3.96$, 3.95 and at most 4.03. This is close to the floor 4 that [CE34] proves for mollified triangle bounds, although the torus minimum is not a bound of that type. These numbers need care. A first round of bisections, with three starts and 200 iterations, was optimistic: with six starts and 400 iterations some values of t that had passed failed (at $X = 10^{11}$, $y = 0.2$, $t = 0.15$ the minimum found dropped from $+0.225$ to -0.073), and the runs with small y (0.05) were discarded for the same reason. If the law $t^* \approx C/\log X$ persists, a bound $\Lambda \le 0.1$ by this route would need X between about 10^{15} and 10^{20}, depending on the fit and on y_0. With the constant 4 in the normalisation of [CE34] it would need $\log(X/4\pi) \approx 40$, that is $X \approx 3 \cdot 10^{18}$, so RH verified to about $1.5 \cdot 10^{18}$, against $3 \cdot 10^{12}$ today. For comparison, the explicit unmollified criterion of [CE34] gives 0.1345 at $X = 10^{20}$. Status: numerical, not certified, from the author's working notes; the optimisation scripts are not among the ancillary files.

Relation to the other papers of the series. The proof of Theorem 1 uses only [Pm], [PT] and the computations of this paper. It uses neither the cross-energy C_2 nor any result of the other papers of the series. What the series supplied is the approach, in three ways.

(1) *Optimising the weights instead of prescribing them.* In Part 18 [CE18] a Dirichlet-polynomial mollifier $M(s) = \sum_{n \le N} a_n n^{-s}$ enters the Jensen moment of ζ through the ratio $R(M) = \int |\zeta M(\frac{1}{2} + it)|^2 d\mu(t)/|M(1)|^2$. There the coefficients are chosen by minimising $R(M)$, a least-squares problem, and not by the Möbius function. That paper also proves that no choice of the coefficients brings $\frac{1}{2}\log R(M)$ below the floor $\frac{1}{2}\log(1 + c_0) = 0.0386$ [CE18, Prop. 46]. Lemma 3 transfers this idea to Polymath's criterion. Here the functional is the concave, piecewise-linear $\mathcal{L}$ instead of a quadratic form, so the optimisation is an ℓ^1 regression. The feature that makes it usable in a proof is that any weights, optimal or not, give a valid bound, so only the evaluation of $\mathcal{L}$ has to be certified.

(2) *The torus of prime phases.* Part 1 [CE1] studies the cross-energy $C_2(N, s) = |X_N(s)|^2 - |X_{N-1}(s)|^2 - N^{-2\sigma} = 2\,\mathrm{Re}\,\big(N^{-\bar{s}} X_{N-1}(s)\big)$ of the partial sums $X_N(s) = \sum_{n \le N} n^{-s}$. Part 6 [CE6] studies the corresponding energy of the primes. Both read these energies through the phases n^{-it}, which by unique factorisation are determined by the prime phases, and Part 6 treats the prime phases as independent under the linear independence hypothesis. The same viewpoint, applied to f_{t_0}, led us to compare Polymath's triangle-inequality bound with the actual minimum of $|f_{t_0}|$ over the torus. The gap is large: at $X \approx 6 \cdot 10^{12}$, $t_0 = 0.13$, $y_0 = 0.2$, the bound is -1.97, while the numerical minimum is $+0.39$. The optimised mollifier closes part of this gap, and the paragraph above on the torus minimum measures what is left.

(3) *Companion results.* Part 34 [CE34] shows that mollified triangle bounds with mollifier

length at most $N/2$ cannot give a constant below 4 in $\Lambda \le C/\log X$; Theorem 1 has $C = 4.68$. Part 35 [CE35] bounds Λ from below in terms of a hypothetical off-line zero. Together they place Theorem 1 between what the method can and cannot reach at this height.

The new contributions of this paper are therefore:

- the optimisation of the mollifier in Polymath's criterion, that is, Lemma 3 for arbitrary weights together with its ℓ^1 formulation;
- the covering of all $x \ge X$ with an explicit tail (Lemmas 6 and 8);
- the certificate, reproduced on two platforms.

Data and code. All the material on which the proof depends is publicly archived in a version-specific record for this version of the paper [1]:

`https://doi.org/10.5281/zenodo.XXXXXXXX`

The archive contains a folder `anc/`, to which every reference to "ancillary files" and "ancillary scripts" in this paper points, and a file `SHA256SUMS.txt` with the hash of every file. It contains:

- the certificate scripts `certify_all.py`, `cert_region_ii.py`, `cert_barrier.py` and `common.py`; `certify_all.py` runs everything, resumes after interruptions and writes a summary with SHA-256 hashes;
- the mollifier weights, `lam_L0174.npy` (240 float64 numbers, used in the proof) and `lam_L0175.npy` (120 numbers, not used in the proof);
- the certificate files `CERTIFICATE_0.174.txt` and `CERTIFICATE_0.174_linux.txt` and the complete logs (`driver.log`, `barrier.log`, `region_ii.log`) of both Arb runs, in the folders `logs_0.174` (Windows 11) and `logs_0.174_linux` (Linux);
- the audit script `audit_lemmas.py`, the float stand-in `mockflint.py` (for tests only), and the scripts for the figures.

A copy of this folder is also included in the source files of this submission, in the file formats the journal accepts. There the weights are stored exactly as text, in `lam_L0174.csv` and `lam_L0175.csv` (shortest round-trip decimal form of each float64 number). The script `restore_weights.py` rebuilds `lam_L0174.npy` and `lam_L0175.npy` from them and checks that they are byte-identical to the files used in the runs (same SHA-256). The certificate files are included unchanged as `CERTIFICATE_0.174.log` and `CERTIFICATE_0.174_linux.log`, the README, archive description and licence are combined in `README.yaml`, and the hashes are listed in `SHA256SUMS.tsv`. The hashes of the inputs of the certificate are listed in Table 6.

The certificate needs Python, numpy and python-flint, and about one hour on a laptop.

Use of AI tools. The computations and the drafting of this paper were carried out with the assistance of an AI system (Claude, Anthropic), under the author's direction. The author checked the results and takes responsibility for them.

A The certification procedure in detail

This appendix lists every step that turns floating-point computations into the inequalities used in the proof of Theorem 1, with the corresponding function of the ancillary scripts in brackets.

A.1 Inputs. The parameters $t_0 = 0.15399$, $y_0 = 0.2$, $X = 5\,998\,313\,329\,980.3135$ are given as decimal strings and converted to Arb balls that contain them. The 240 weights are stored as float64 numbers (`lam_L0174.npy`); a float64 number is an exact dyadic rational, so the weights are exact inputs and no rounding of the optimisation enters. The scripts check $\lambda_1 = 1$.

A.2 From balls to floats. Every transcendental quantity ($\log n$, $e^{\frac{t}{4}\log^2 n}$, $n^{-\sigma}$, d^{-y}, $\sqrt{x/4\pi}$, the phases, the complex logarithms in α and M_0) is computed with Arb at 96 bits (hypothesis (ii)) or 128 bits (hypothesis (iii)). A ball $[m \pm r]$ is converted to the float interval obtained by rounding $m-r$ and $m+r$ to the nearest float and then moving one more ulp outward [`common.lo`, `common.hi`].

A.3 Large sums. The sums over $n \le DN \approx 1.7 \cdot 10^8$ (and, in later chunks, up to $5 \cdot 10^8$) are formed in float64 from interval data, using only $+, -, \times$. Under IEEE-754 rounding to nearest, the exact result of one operation on floats lies within half an ulp of the computed one, so moving the result one ulp outward gives a valid enclosure [`dn`, `up`, `rmul_pos`]. A sum of n nonnegative floats computed in any order differs from the exact sum s by at most $\gamma_{n-1}s$ with $\gamma_n = nu/(1-nu)$, $u = 2^{-53}$ [Hi, Sect. 4.2], so $\hat{s}(1+2\gamma_n)$, rounded up, is an upper bound [`sum_up`].

A.4 The coefficients. For each n the coefficients c_n and $c_n'(y_a)$ are accumulated as intervals over the pairs (d, m), $dm = n$, from the intervals for b_m and d^{-y_a}; $|c_n|$ is bounded by the larger endpoint in absolute value. The correction η_n of Section 4 is accumulated with upward rounding, using $D^{k(x)} - 1 \le 10^{-12}$. In fact $D^{k(x)} - 1 \le 7.1 \cdot 10^{-14}$ for $x \ge X$ [`main_sum`].

A.5 Monotone factors on blocks. The weights $n^{-\sigma_a}$ and n^e (with $e < 0$, checked) decrease in n. They are replaced by their values at the left end of geometric blocks $[B_k, B_{k+1})$ of ratio $1+2^{-13}$, exact for $n < 4096$. Since $\sigma_a \approx 1.64$, the cost is a relative loss below $2.1 \cdot 10^{-4}$ [`geom_blocks`].

A.6 The error terms. For hypothesis (ii) we use (23) and (24) of [Pm] with the following explicit simplifications, all valid for $x \ge X$ and $y_0 \le y \le y_b = 0.831877$:

- $|\gamma| N^{|\kappa|} n^y \le e^{0.02} \cdot 1.0001$, since $N \le \sqrt{x/4\pi} + \frac{t}{16}$;
- $\log^2 \frac{x}{4\pi n^2} \le \log^2 \frac{x}{4\pi}$ for $1 \le n \le N$;
- $1.24(3^y + 3^{-y}) \le 1.24(3y_b + 1)$, since $3^y + 3^{-y} \le 2.90 < 3.50$.

For the barrier we use $3^y + 3^{-y} \le 4$ on $[0, 1]$. Every factor of the resulting bounds is non-increasing in x, and the sum $\sum_{n \le N(x)} b_n n^{-\operatorname{Re} s_*}$ in (23) is bounded uniformly in $x \ge X + \sqrt{1-y_0^2}$ by its value at that point plus the tail of Lemma 8, because $F(m)$ dominates the new term $b_m m^{-\sigma_a(x_m)}$ (the summand $d = 1$, $\lambda_1 = 1$). The result is $e_A + e_B + e_{C,0} \le 2.977 \cdot 10^{-7}$ [`errors_majorant`].

A.7 Chunks and tail. On each y-interval the chunk end N_b is chosen by a floating-point estimate, which is not part of the proof. The sum $\sum_{N_a < m \le N_b} F(m)$ is then bounded rigorously by Lemma 6(b), with blocks of ratio $1 + 2^{-9}$ [`extra`]. The script evaluates F with the factor $D^{k(x_v)}$ replaced by its upper bound $1 + 10^{-12}$, valid for all $v \ge N(X)$; since the function F of the lemma is decreasing and is bounded by the script's values at the block starts, the block bound remains valid [`F_arb`]. The last chunk uses Lemma 8, with steps $v_{j+1} = 1.01 v_j$ up to e^{60} and the check $F(e^{60})e^{120} < 1$; the actual values are about $4 \cdot 10^{-24}$ [`future_tail`]. Table 5 lists the chunks of the hardest y-interval.

x_a	N_a	$\mathcal{L}_{N_a}(x_a) \geq$	$\sum F \leq$ (chunk or tail)	$M^+(x_a) \leq$	$\lvert f_{t_0}\rvert \geq$
$5.998 \cdot 10^{12}$	690 891	0.02188	0.01021	1.9646	0.00594
$6.149 \cdot 10^{12}$	699 527	0.02864	0.01012	1.9630	0.00943
$6.304 \cdot 10^{12}$	708 270	0.03535	0.01889	1.9614	0.00839
$6.607 \cdot 10^{12}$	725 089	0.04792	0.01858	1.9585	0.01498
$6.924 \cdot 10^{12}$	742 307	0.06035	0.03083	1.9555	0.01509
$7.498 \cdot 10^{12}$	772 457	0.08113	0.04766	1.9505	0.01715
$8.520 \cdot 10^{12}$	823 384	0.11361	0.06963	1.9425	0.02264
$1.038 \cdot 10^{13}$	908 917	0.16192	0.09614	1.9304	0.03407
$1.399 \cdot 10^{13}$	1 055 107	0.23048	0.12408	1.9125	0.05563
$2.173 \cdot 10^{13}$	1 314 924	0.32263	0.19768	1.8870	0.06621
$5.332 \cdot 10^{13}$	2 059 906	0.48053	0.43661 (tail)	1.8382	0.02389

Table 5: The 11 chunks for $y \in [0.200, 0.205]$ (log `region_ii.log`). The last column is $(\mathcal{L}_{N_a}(x_a) - \sum F)/M^+(x_a)$, recomputed here from the rounded entries of the log (the script uses the unrounded values); the last chunk covers all $x \geq 5.332 \cdot 10^{13}$. The minimum, 0.00594, is the entry of Table 3.

A.8 The barrier: evaluation of f_t. On $X \leq x \leq X+1$ the truncation $N = 690\,891$ is constant (checked with Arb), so f_t is holomorphic in $z = x + iy$. Following [Pm, Sect. 7], $n \leq N$ is split into dyadic blocks $[n_0, 2n_0)$, and $\log n = \log n_0 + u$ with $0 \leq u < \log 2$. The dependence on (x, y, t) is expanded around the centre $x_c = X + \frac{1}{2}$, $y_c = 0.6$ in powers of u, to order 44 in the linear part and order 10 in the quadratic part $\frac{t}{4}u^2$. The moments $\sum_n n^{-(1\pm y_c)/2} e^{\pm i \frac{x_c}{2} \log n} u^j$ are computed once, with the phases $\frac{x_c}{2} \log n \bmod 2\pi$ evaluated in Arb at 128 bits. Since $\frac{x_c}{2} \log n < 5 \cdot 10^{13} < 2^{46}$, about 80 bits remain after the reduction. The remainders of both truncated series are bounded by $\frac{(cu)^{45}}{45!} e^{cu+w} + \frac{w^{11}}{11!} e^{w+cu}$, with $|c|u$ and $w = \frac{t}{4}u^2$ bounded above in Arb, and added to the enclosure. The Taylor values agree with direct summation to 10^{-15} [`f_eval`, `coef`].

A.9 The barrier: derivative bounds and Rouché. The bounds D_z and D_t are those of [Pm, Lemma 8.4]. They are evaluated on geometric blocks of ratio $1 + 2^{-10}$, using, on a block $[n_0, n_1]$, the value of $b_n n^{-\operatorname{Re} s_*}$ at n_0 and the value of $\log n$ at n_1. This is valid because $b_n n^{-\operatorname{Re} s_*}$ decreases in n. For $n \leq N$, it also decreases in t: its exponent is $-\frac{1+y}{2} \log n + \frac{t}{4} \log n \, (\log n - \log \frac{x}{4\pi})$ and $\log n < \log \frac{x}{4\pi}$. So the value at the left end t_1 of a time step bounds it on the whole step. Likewise, $|\gamma| n^y n^{-\operatorname{Re} s_*}$ decreases in y, so the lowest y of the rectangle is the worst case [`bounds`].

For each step $[t_1, t_2]$ the script checks four things on a closed mesh $\{z_j\}$ of ∂R with maximal spacing h (computed exactly):

- $\min_j |f_{t_1}(z_j)| > D_z h$, so that f_{t_1} has no zero between consecutive mesh points;
- $\operatorname{Re}\big(f_{t_1}(z_{j+1})\overline{f_{t_1}(z_j)}\big) > 0$ for all j, in interval arithmetic, so that every increment of $\arg f_{t_1}$ lies in $(-\frac{\pi}{2}, \frac{\pi}{2})$;
- the sum of the increments, computed from the centres of the enclosures plus the error bound $\frac{\pi}{2}(r_j/m_j + r_{j+1}/m_{j+1})$ per term and a slack of 10^{-6} per term for the library function `angle`, is less than π in absolute value. Hence the winding number is 0, and f_{t_1} has no zero in R;
- $\min_j |f_{t_1}(z_j)| - \frac{D_z h}{2} - D_t(t_2 - t_1) - E > 0$. Then $|H_t/B_t - f_{t_1}| < |f_{t_1}|$ on ∂R for every $t \in [t_1, t_2]$, and by Rouché's theorem H_t/B_t has no zero in R.

The steps run from $t = 0$ to a float $\geq t_0$. The value $t = 0$ itself is covered by hypothesis (i), since $(X+1)/2 < 3 \cdot 10^{12}$ [main loop of `cert_barrier.py`].

A.10 Fail-safe design. Every check above is an `assert`. A failed check stops the program, and the line `CERTIFIED` is printed only after all checks have passed. The driver `certify_all.py` refuses to combine logs produced by different versions of the scripts. It also checks that the certified y-intervals cover $[y_0, \sqrt{1-2t_0}]$ without gaps, and it writes the SHA-256 hashes of all inputs into the certificate file.

B Reproducibility

Table 6 lists the files on which Theorem 1 depends. The hashes are those printed by both certificate runs and recomputed from the archived files [1].

file	SHA-256
`lam_L0174.npy`	`d71b379ee04a299191ec31c420d4dcca6bba3fc61c707eb9ee4c71c0c49b1235`
`cert_region_ii.py`	`8ca106d8a5609d7f093529cdb1614f5da773bdb78484afd30dba4dc5a481c4ec`
`cert_barrier.py`	`1882d2ce112ed1a551cff3d1ec4d7d131c2bfd46b628ec1b9cde8993921ea4fe`
`common.py`	`22361af17deaffa7c7761367f84cc90bc7dbf44d44267e32ab5ddc5273211e18`
`certify_all.py`	`a2ae5bc2137d4b96ce49e262a68c7ef1a58f0cdd9f0cfe12b5e09f461da1251a`

Table 6: Inputs of the certificate.

Second run on a different platform. The unchanged scripts and weights (same hashes) were run a second time, on 20 October 2026, on a different platform. The first run, which produced the tables of this paper, used Windows 11, Python 3.13.2, numpy 2.4.2 and the python-flint 0.9.0 wheel. The second used Linux (glibc 2.39), Python 3.13.16, numpy 2.5.3 and python-flint 0.9.0 compiled from source against FLINT 3.6.0, GMP 6.3.0 and MPFR 4.2.2. Apart from the timings, the two runs printed identical output: all 73 barrier steps with their bounds and margins, the bound $2.977 \cdot 10^{-7}$ for the error terms, and the 7 y-intervals of hypothesis (ii) with all their chunks. The second run took 53 minutes; its logs and certificate file are `logs_0.174_linux` and `CERTIFICATE_0.174_linux.txt`.

Correspondence with the text.

- Lemma 3, Remark 4 and the definition of $\mathcal{L}_{N'}$: `main_sum`, which returns $\mathcal{L}_{N_a}(x_a)$ and $M^+(x_a)$.
- Lemma 6(a): the chunk loop in the main program of `cert_region_ii.py`.
- F and Lemma 6(b): `F_arb` and `extra`.
- Lemma 8: `future_tail`.
- The error terms of A.6: `errors_majorant`.
- Section 5 and A.8–A.9: `cert_barrier.py`.

The audit script `audit_lemmas.py`, which is not part of the certificate, checks the hashes, the algebra of Lemma 3 at exact values of s_*, κ, γ, the side conditions of A.4 and A.6, and the signs of the derivative bounds in the proofs of Lemmas 6 and 8. It also recomputes $\mathcal{L}_{N_a}(x_a)$ at the first chunk in plain floating point, independently of `main_sum`, obtaining 0.02195 against the certified 0.02188.

References

[Arb] F. Johansson, Arb: efficient arbitrary-precision midpoint-radius interval arithmetic, *IEEE Trans. Comput.* 66 (2017), 1281–1292.

[BS] E. Balanzario and J. Sánchez-Ortiz, Zeros of the Davenport–Heilbronn counterexample, *Math. Comp.* 76 (2007), 2045–2049.

[DH] H. Davenport and H. Heilbronn, On the zeros of certain Dirichlet series I, II, *J. London Math. Soc.* 11 (1936), 181–185 and 307–312.

[dB] N. G. de Bruijn, The roots of trigonometric integrals, *Duke Math. J.* 17 (1950), 197–226.

[Gor] S. Gordon, A computer-assisted upper bound for the de Bruijn–Newman constant, preprint and code (2026), `https://github.com/stefangordon/dbn-upper-bound`; not peer reviewed.

[Hi] N. J. Higham, *Accuracy and Stability of Numerical Algorithms*, 2nd ed., SIAM, Philadelphia, 2002.

[HB] C. Hakimoglu-Brown, A conditional bound $\Lambda \leq 0.13963$ for the de Bruijn–Newman constant, preprint (2026), arXiv:2610.12803.

[Go] J. Gomila, de Bruijn–Newman constant: $\Lambda \leq 0.1787854$, online announcement and audit repository (August 2026), `https://judegomila.com/posts/riemann-lambda-0.1787854`; not peer reviewed.

[KKL] H. Ki, Y.-O. Kim and J. Lee, On the de Bruijn–Newman constant, *Adv. Math.* 222 (2009), 281–306.

[Mu] GitHub user DrMurphyIsIn, A kernel-checked bound $\Lambda \leq 9/32$ for the de Bruijn–Newman constant from the quasi-Riemann hypothesis, Lean 4 repository (2026), `https://github.com/DrMurphyIsIn/qrh-debruijn-newman`.

[Ne] C. M. Newman, Fourier transforms with only real zeros, *Proc. Amer. Math. Soc.* 61 (1976), 245–251.

[OAI] OpenAI, manuscript claiming a zero-free half-plane $\operatorname{Re} s > \frac{7}{8}$ for ζ and Dirichlet L-functions, dated 30 September 2026, released 6 October 2026, with a partial Lean formalization, `https://github.com/openai/math`; not peer reviewed.

[Pl] M. Planat, A certified classical-strip comparison for the de Bruijn–Newman constant, preprint (2026), arXiv:2610.18214.

[PT] D. Platt and T. Trudgian, The Riemann hypothesis is true up to $3 \cdot 10^{12}$, *Bull. London Math. Soc.* 53 (2021), 792–797; arXiv:2004.09765.

[Pm] D. H. J. Polymath, Effective approximation of heat flow evolution of the Riemann ξ function, and a new upper bound for the de Bruijn–Newman constant, *Res. Math. Sci.* 6 (2019), 31; arXiv:1904.12438.

[RT] B. Rodgers and T. Tao, The de Bruijn–Newman constant is non-negative, *Forum Math. Pi* 8 (2020), e6.

[CE1] P. Caceres, Cross-Energy of Dirichlet Partial Sums. Part 1: The C-transform and the cross-energy, preprint, 2026.

[CE6] P. Caceres, Cross-Energy of Dirichlet Partial Sums. Part 6: Second-order asymptotics and limiting fluctuations of the prime energy, preprint, 2026.

[CE18] P. Caceres, Cross-Energy of Dirichlet Partial Sums. Part 18: The Euler–Caceres bound, preprint, 2026.

[CE34] P. Caceres, Cross-Energy of Dirichlet Partial Sums. Part 34: The constant in the $C/\log X$ law for triangle-inequality upper bounds on the de Bruijn–Newman constant, preprint, 2026.

[CE35] P. Caceres, Cross-Energy of Dirichlet Partial Sums. Part 35: How long can an off-line zero survive the de Bruijn–Newman heat flow? An explicit lower bound for Λ forced by a zero off the critical line, preprint, 2026; an earlier version is hexagon:2610.00207.

[1] P. Caceres, *Proof material for "Optimised mollifiers and the bound $\Lambda \leq 0.174$ for the de Bruijn–Newman constant" (version 3): mollifier weights, certificate scripts and complete certificate logs*, Zenodo, 2026, `https://doi.org/10.5281/zenodo.XXXXXXXX`.